Structural and electron charge density studies of a nonlinear optical compound 4,4 di-methyl amino cyano biphenyl

Naima Boubegra, Abdelkader Chouaih†, Mokhtaria Drissi, and Fodil Hamzaoui

Laboratoire de Technologie et Propriétés du Solide (LTPS), Université Abdelhamid Ibn Badis de Mostaganem, 27000 Mostaganem, Algeria

(Received 25 March 2013; revised manuscript received 29 June 2013; published 3 December 2013)

The 4,4 dimethyl amino cyano biphenyl crystal (DMACB) is characterized by its nonlinear activity. The intra molecular charge transfer of this molecule results mainly from the electronic transmission of the electro-acceptor (cyano) and electro-donor (di-methyl-amino) groups. An accurate electron density distribution around the molecule has been calculated based on a high-resolution X-ray diffraction study. The data were collected at 123 K using graphite-monochromated Mo $K\alpha$ radiation to $\sin(\theta)/\lambda = 1.24$ Å^{-1}. The integrated intensities of 13796 reflections were measured and reduced to 6501 independent reflections with $I \geq 3\sigma(I)$. The crystal structure was refined using the experimental model of Hansen and Coppens (1978). The crystal structure has been validated and deposited at the Cambridge Crystallographic Data Centre with the deposition number CCDC 876507. In this article, we present the thermal motion and the structural analysis obtained from the least-square refinement based on F^2 and the electron density distribution obtained from the multipolar model.

Keywords: electron charge density, 4,4 dimethyl amino cyano biphenyl crystal (DMACB), multipolar refinement

PACS: 61.66.Hq, 42.65.–k, 31.15.A–, 71.20.–b **DOI:** 10.1088/1674-1056/23/1/016103

1. Introduction

In the nonlinear optical (NLO) field, organic molecular crystals have attracted much interest mainly because of their optical transparency and optical efficiency, which can be superior by several orders of magnitude to those of the best known mineral materials. Among them, organic second-order NLO molecules have been widely investigated by experimental and theoretical chemists due to their high electro-optic (EO) coefficients, facile processing, as well as low dielectric constants.[1–5] These molecules are prepared with suitable donor-acceptor (D, A) couples connected by a transmitter group T (π-electron). These kinds of molecules are known under the term push-pull molecules.[6–10] A typical organic compound consists of strong electron acceptors (e.g. NO_2 or CN groups) and donors (e.g. NR_2 or OR groups) connected by a π-conjugated system. This arrangement ensures efficient intramolecular charge transfer and enables further fine-tuning of the polarisability of the compound.[11–14]

The 4,4 di-methyl amino cyano biphenyl compound (DMACB) is considered to be one of the most interesting materials in non-linear optics because it crystallizes readily compared to other competitive crystals. A structural analysis has been already carried out at room temperature by Zyss *et al.*[15] The DMACB crystallizes in the noncentrosymmetric space group *Cc* with four molecules in the unit cell. Its structure is shown in Fig. 1.

This work focuses on the thermal motion analysis and the electronic charge density distribution of the DMACB molecule using high-resolution X-ray diffraction data performed at 123 K. To achieve this study, we used the XD program package based on the Hansen–Coppens charge density model.[16] One major component of this package is a program for the least-square fitting of the experimental data.[17]

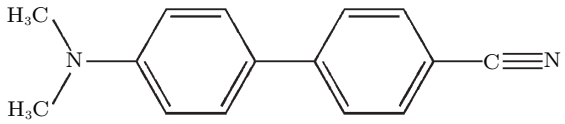

Fig. 1. Chemical structure of DMACB.

2. Experiment

The crystallographic data were obtained at 123 K on a CAD4 diffractometer using the graphite–monochromated Mo $K\alpha$ radiation. A crystal of dimensions 0.2 mm×0.2 mm×0.15 mm was used for the data collection. The crystal of high quality was cooled using a modified Enraf Nonius nitrogen gas-flow system. The cell parameters were determined from refinement by using the centered angular positions of 25 reflections with $11 \leq \theta \leq 25°$. The profiles of the different reflections were measured using the θ–2θ step scan method. A total of 13796 intensities were recorded up to 2θ of 59.7°. Only selected reflections with significant intensities were collected in the high-order θ range. The data merged to give 6501 independent reflections. Only 5729 reflections for which $I \geq 3\sigma(I)$ were used for the refinement.

The H atoms were located by difference Fourier synthesis. The data reduction and error analysis were carried out by using the program of Blessing (1989).[18] The experimental

†Corresponding author. E-mail: achouaih@gmail.com

details and crystal data are displayed in Table 1. The crystal structure has been validated and deposited at the Cambridge Crystallographic Data Centre with the deposition number CCDC 876507. The full details can be obtained free of charge from the Cambridge Crystallographic Data Centre.

Table 1. Experimental details.

Crystal data	
Chemical formula	$C_{15}H_{14}N_2$
Chemical formula weight	222
Cell setting	monoclinic
Space group	*Cc*
a/Å	9.503 ± 2
b/Å	16.429 ± 6
c/Å	8.954 ± 4
β/(°)	122.040 ± 3
V/Å^3	1185.01 ± 8
Z	4
D_x/mg·m^{-3}	1.40 ± 01
Radiation type	Mo $K\alpha$
Wavelength/Å	0.71073
No. of reflections for cell parameters	25
θ range/(°)	2–29.6
μ/cm^{-1}	0,69
Temperature/K	123 (1)
Crystal form	prism
Crystal size/mm	0.2 × 0.2 × 0.15
Crystal color	coulorless
Data collection	
Diffractometer	Nonius CAD-4
Data collection method	θ–2θ
$2\theta_{max}$	59.7
No. of measured reflections	13796
No. of independent reflections	6501
No. of observed reflections	5729
Criterion for observed reflections	$I \geq 3\sigma(I)$
R_{int}	0.018
Range of h, k, l	$0 \rightarrow h \rightarrow 11$
	$0 \rightarrow k \rightarrow 12$
	$-12 \rightarrow l \rightarrow 12$
No. of standard reflections	3
Frequency of standard reflections	every 60 min

3. Refinement

In addition to the conventional least-square refinement of data sets, a separate refinement using only high-order reflections ($\sin\theta/\lambda \geq 0.75$ Å^{-1}) was performed. For this latter set of reflections, the X-ray scattering was mainly from the core electrons. The high-order data were expected to yield atomic parameters less biased by the inadequacy of the spherical-atom model. We continued our refinement using the XD program based on the Hansen–Coppens charge density model, in which the atomic density is described as a series expansion in real spherical harmonic functions Y_{lm} up to order four[15]

$$\rho_i = p_{i,c}\rho_{i,c} + p_{i,v}\kappa^3\rho_{i,v}(\kappa_i r_i) + \sum_{I=0}^{4} k'^3 R_{k,l}(k'', r) + \sum_{m=-1}^{l} P_{k,lm} Y_{lm}^k \frac{r}{|r|}, \quad (1)$$

where ρ_c and ρ_v are spherically averaged Hartree–Fock core and valence densities, with ρ_v normalized to one electron, Y_{lm} are multipolar spherical harmonic angular functions in real form, $R_l = N_l r^n \exp(-k'\xi r)$ are Slater–type radial functions with N_l as the normalization factor and $n = n(l)$ and ξ being parameters chosen according to the criteria given by Hansen and Coppens.[15] The development was trunked to the third order $l_{max} = 3$ and the coefficients of the hexadecapole functions ($l = 4$) were constrained to be zero. The coefficients of the radial functions were $n_1 = 2, 2, 3$ (for $l = 1, 2, 3$, respectively) for non–H atoms and $n_1 = l$ for H atoms.

The adjustable variables were the valence-shell contraction–expansion parameters k', k'', the population parameter P_v and the multipolar parameters P_{lm}. To reduce the number of variables, chemical constraints were imposed, with which atoms of similar environment were assumed to have the same deformation.

The scattering factors for the non-H atoms were taken from the international tables for X-ray crystallography.[19] The scattering factors of the H atoms were those of Stewart *et al.*[20] The results of this refinement are summarized in Table 2. An isotropic extinction correction as described by Becker and Coppens was applied.[21]

Table 2. Least-square refinement factors, where N is the number of refined parameters, $R = \sum||F_o| - |F_c||/\sum|F_o|$, $wR = [\sum w(|F_o| - |F_c|)^2/\sum w|F_o|^2]^{1/2}$, $S = [\sum w(|F_o| - |F_c|)^2/(M-N)]^{1/2}$; the atomic scattering factors come from the international tables for X-ray crystallography.[19]

Spherical refinement	N	R	wR	S
	195	0.028	0.026	1.02

4. Structural analysis

In order to investigate the theoretical calculations of the molecular structure parameters, we have applied *ab intio* methods. These calculations were performed with the density functional theory (DFT) at B3LYP (Becke's three parameter hybrid functional using the correlation functional of Lee, Yang and Parr, which includes both local and non-local terms in the correlation functional) method at the 6-31G* level using the Gaussian 03 computational chemistry program package.[22] The parameters of the optimized structure (bond lengths and bond angles) are listed in Tables 3 and 4. It can be seen that all the calculated parameters are in accordance with the X-ray results. In spite of the differences, the calculated geometric parameters represent a good approximation and can provide a starting point to calculate other parameters, such as vibrational wavenumbers, as will be described in the next work.

Table 3. Bond lengths of DMACB in units of Å, with estimated deviations in parentheses.

Atom 1	Atom 2	Distance		Atom 1	Atom 2	Distance	
		X-ray	DFT			X-ray	DFT
N(1)	C(13)	1.144 (3)	1.137	C(4)	C(5)	1.374 (3)	1.381
N(2)	C(10)	1.372 (3)	1.410	C(5)	C(6)	1.401 (3)	1.394
N(2)	C(14)	1.435 (3)	1.453	C(6)	C(7)	1.468 (3)	1.488
N(2)	C(15)	1.436 (4)	1.445	C(7)	C(8)	1.393 (4)	1.395
C(1)	C(2)	1.377 (3)	1.381	C(7)	C(12)	1.393(3)	1.386
C(1)	C(6)	1.397 (4)	1.394	C(8)	C(9)	1.382 (3)	1.377
C(2)	C(3)	1.384 (4)	1.390	C(9)	C(10)	1.393 (3)	1.398
C(3)	C(4)	1.391 (4)	1.390	C(10)	C(11)	1.394 (4)	1.387
C(3)	C(13)	1.438 (3)	1.444	C(11)	C(12)	1.382 (3)	1.391

Table 4. Bond angles of DMACB in units of (°), with estimated deviations in parentheses.

Atom 1	Atom 2	Atom 3	Angle		Atom 1	Atom 2	Atom 3	Angle	
			X-ray	DFT				X-ray	DFT
C(10)	N(2)	C(14)	120.9 (3)	116.0	C(1)	C(6)	C(5)	117.6 (2)	116.0
C(10)	N(2)	C(15)	121.2 (2)	117.3	C(1)	C(6)	C(7)	121.1 (2)	119.3
C(14)	N(2)	C(15)	117.9 (2)	112.3	C(5)	C(6)	C(7)	121.2 (2)	121.3
C(2)	C(1)	C(6)	121.4 (2)	121.0	C(6)	C(7)	C(8)	121.6 (2)	121.0
C(1)	C(2)	C(3)	119.9 (2)	120.1	C(6)	C(7)	C(12)	121.8 (3)	119.9
C(2)	C(3)	C(4)	119.9 (2)	121.0	C(8)	C(7)	C(12)	116.6 (2)	116.8
C(2)	C(3)	C(13)	120.2 (3)	118.4	C(7)	C(8)	C(9)	121.9 (2)	120.1
C(4)	C(3)	C(13)	119.8 (2)	120.8	C(8)	C(9)	C(10)	121.3 (3)	121.0
C(3)	C(4)	C(5)	119.8 (2)	120.8	N(2)	C(10)	C(9)	121.5 (3)	120.8
C(4)	C(5)	C(6)	121.3 (2)	117.4	N(2)	C(10)	C(11)	121.6 (2)	121.2
C(7)	C(12)	C(11)	121.8 (3)	119.2	C(9)	C(10)	C(11)	116.9 (2)	117.0
N(1)	C(13)	C(3)	180.0 (1)	180.0	C(10)	C(11)	C(12)	121.4 (2)	120.4

It is worth noting that some of the optimized bond lengths and bond angles have slightly different values from the corresponding experimental ones due to the fact that the theoretical calculations consider only isolated molecules in the gaseous phase while the experimental results refer to molecules in a crystal environment.

The general features of the structure at room temperature have been described previously. The DMACB is a non-planar molecule. The dihedral angle between the two phenyl groups is 42°. The main characteristic of this structure is that the four molecules in the unit cell are engaged in four chains formed by infinite chains of hydrogen-bonded coplanar molecules, as shown in Fig. 2. Our results have not been subject to any structural changes compared to the initial published results.

The design of the most efficient organic materials for the non-linear optical (NLO) effect is based on molecular units containing highly delocalized π-electron moieties and extra electron donor (D) and electron acceptor (A) groups on the opposite sides of the molecule at appropriate positions on the ring to enhance the conjugation. The π-electron cloud movement from donor to acceptor makes the molecule highly polarized. The DMACB molecule is designed using acceptor group N≡C– (cyano group), which has the highest acceptor ability, and donor group –$N(CH_3)_2$ (dimethyl amino group) that has the highest donor character. The *ab initio* optimization in this investigation shows that the molecule of DMACB is almost planer. The planarity can affect the NLO properties of DMACB due to the free rotation of two benzene rings. The DMACB molecule has two benzene rings connected through a single covalent bond C–C, which can eventually stop the free rotation and facilitate the intramolecular charge transfer. To understand this phenomenon in the context of the molecular orbital picture, the highest occupied molecular orbitals (HOMOs) and the lowest unoccupied molecular orbitals (LUMOs) should be examined.

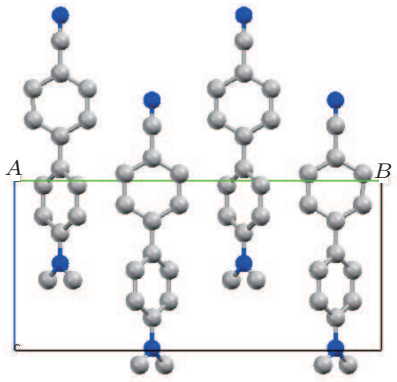

Fig. 2. (color online) Packing diagram of the structure.

5. Thermal motion analysis

The thermal motion analysis of DMACB has been performed using the THMA11 program.[23] The rigid-body mo-

tion is described by three tensors, $\boldsymbol{T}$ for the translation, $\boldsymbol{L}$ for the liberation and $\boldsymbol{S}$ for taking into account the correlation between translation and liberation. These tensors are obtained by a least-square fit refinement using the observed atomic thermal motion parameters obtained by the refinement and given in Table 5. This test indicates that the differences between the mean-square displacement amplitudes (MSDAs) along the interatomic directions have a magnitude $\Delta \leq 10.10^{-4}$ Å^2 for the most bonded pairs of the non-H atoms.[24] The MSDAs Δ_{AB} in the AB direction for all pairs of atoms in the molecule have been calculated and reported in Table 6.

In the general treatment of the molecular thermal motion in terms of rigid-body ($\boldsymbol{TLS}$), the calculated anisotropic thermal parameters are given in the Trueblood notation, such as

$$U_{ij} = T_{ij} + G_{ijkl}L_{kl} + H_{ijkl}S_{kl} + D^2\Omega^2 n_i n_j, \qquad (2)$$

where $\boldsymbol{G}$, $\boldsymbol{H}$ and D are geometrical parameters. The last term corresponds to any additional intra-libration (Ω) around a chosen axis. The rigid-body fit suggests two independent liberation axes around bonds C(10)–N(10) and C(7)–C(6). The thermal motion of the H atoms is considered to consist of two contributions. The first is due to the rigid molecular motion and the second is from the C–H vibrations.[25–27] The $\boldsymbol{T}$, $\boldsymbol{L}$ and $\boldsymbol{S}$ obtained from the least-square fitting are given in Table 7.

The C–H bond frequencies of the molecule were taken from Baert *et al*.[28] The corresponding mean-square displacements for the H atoms in phenyl group were 0.0056 Å^2, 0.014 Å^2 and 0.025 Å^2 for bond stretching, in-plane bending and out-of-plane bending, respectively. While, for the H atoms of the methyl group, the internal vibration amplitudes used were 0.0057 Å^2, 0.0116 Å^2 and 0.0224 Å^2. The results of the thermal motion parameters of the H atoms are summarized in Table 8. The ellipsoids of the different atoms representing their thermal motion described above are shown, using the ORTEPIII[29] diagram, in Fig. 3.

Table 5. Atomic displacement parameters in units of Å^2.

Atom	U_{11}	U_{22}	U_{33}	U_{12}	U_{13}	U_{23}
N(1)	0.0331 (10)	0.0392 (11)	0.0148 (7)	0.0026 (8)	0.0081 (7)	− 0.0006 (7)
N(2)	0.0164 (7)	0.0286 (9)	0.0102 (5)	− 0.0055 (5)	0.0053 (5)	− 0.0005 (5)
C(1)	0.0176 (7)	0.0156 (7)	0.0127 (6)	− 0.0006 (5)	0.0077 (5)	0.0008 (5)
C(2)	0.0169 (7)	0.0155 (7)	0.0143 (6)	− 0.0014 (5)	0.0070 (6)	0.0003 (5)
C(3)	0.0164 (7)	0.0187 (7)	0.0103 (6)	− 0.0002 (5)	0.0056 (5)	− 0.0002 (5)
C(4)	0.0174 (7)	0.0164 (7)	0.0134 (6)	− 0.0020 (5)	0.0071 (5)	− 0.0019 (5)
C(5)	0.0183 (7)	0.0143 (6)	0.0131 (6)	− 0.0021 (5)	0.0075 (5)	− 0.0005 (5)
C(6)	0.0148 (7)	0.0144 (7)	0.0128 (6)	− 0.0010 (5)	0.0073 (5)	− 0.0002 (5)
C(7)	0.0149 (7)	0.0137 (6)	0.0120 (6)	− 0.0012 (5)	0.0068 (5)	0.0000 (5)
C(8)	0.0142 (6)	0.0202 (7)	0.0134 (6)	− 0.0034 (5)	0.0067 (5)	0.0001 (5)
C(9)	0.0161 (7)	0.0182 (7)	0.0139 (6)	− 0.0032 (5)	0.0083 (5)	− 0.0001 (5)
C(10)	0.0134 (6)	0.0151 (6)	0.0123 (5)	− 0.0006 (4)	0.0062 (5)	− 0.0005 (5)
C(11)	0.0170 (7)	0.0193 (7)	0.0120 (6)	− 0.0034 (5)	0.0075 (5)	0.0006 (5)
C(12)	0.0155 (7)	0.0186 (7)	0.0131 (6)	− 0.0035 (5)	0.0068 (5)	0.0001 (5)
C(13)	0.0192 (8)	0.0200 (8)	0.0144 (7)	0.0024 (6)	0.0075 (6)	0.0009 (6)
C(14)	0.0159 (7)	0.0278 (8)	0.0139 (6)	− 0.0018 (6)	0.0056 (5)	− 0.0005 (6)
C(15)	0.0203 (7)	0.0271 (8)	0.0140 (6)	− 0.0010 (6)	0.0101 (6)	0.0017 (6)

Table 6. Matrix for differences in MSDAs (mean square displacements of atoms). Values listed are 10^4 MSDAs for column atom minus that for row atom, underlined values correspond to chemical bonds.

	C15	C14	C13	C12	C11	C10	C9	C8	C7	C6	C5	C4	C3	C2	C1	N2
N1	−4	4	13	−4	−6	−12	−4	−6	2	−7	−16	−17	−12	−15	−4	−16
N2	1	22	29	4	5	4	28	10	19	9	26	8	5	9	16	
C1	−5	−1	15	−4	13	−17	−7	11	−8	4	−9	2	−6	7		
C2	2	9	20	5	−2	−9	1	13	3	−3	−17	15	8			
C3	13	17	25	12	9	−1	10	12	14	4	−10	8				
C4	12	14	−2	15	10	−4	7	8	12	15	10					
C5	−4	−4	15	3	−11	−24	−10	−7	−14	9						
C6	8	10	20	4	0	−5	5	19	10							
C7	−5	1	11	5	−6	−14	−10	17								
C8	10	12	14	−12	−2	−5	6									
C9	5	−7	15	5	3	13										
C10	−6	16	25	−4	4											
C11	−8	11	16	1												
C12	1	9	13													
C13	−12	−6														
C14	−7															

Table 7. Rigid body vibration parameters of the $\boldsymbol{T}$, $\boldsymbol{L}$ and $\boldsymbol{S}$ tensors.

$\boldsymbol{T}$ (rad^2)			$\boldsymbol{L}$ (Å^2)			$\boldsymbol{S}$ (rad Å)		
0.00136			0.01089			0.00029	−0.00001	0.00000
0.00006	0.00037		0.00203	0.01029		0.00015	−0.00038	0.00010
−0.00008	−0.00005	0.00044	−0.00031	−0.00013	0.01289	0.00014	0.00003	0.00000

Table 8. The thermal vibration parameters for the H atoms calculated from the $\boldsymbol{TLS}$ group tensors plus the internal C–H bond vibration.

Atom	U_{11}	U_{22}	U_{33}	U_{12}	U_{13}	U_{23}
H(1)	0.0307	0.0134	0.0163	0.0005	0.0058	0.0009
H(2)	0.0352	0.0188	0.0163	0.0002	0.0072	0.0010
H(3)	0.0322	0.0190	0.0138	−0.0035	0.0047	−0.0050
H(5)	0.0255	0.0141	0.0136	−0.0026	0.0035	−0.0038
H(8)	0.0150	0.0272	0.0130	−0.0061	0.0032	−0.0016
H(9)	0.0212	0.0307	0.0131	−0.0059	0.0040	−0.0011
H(11)	0.0188	0.0273	0.0183	−0.0085	0.0012	−0.0049
H(12)	0.0180	0.0261	0.0183	−0.0091	0.0045	−0.0035
H(14A)	0.0154	0.0405	0.0189	−0.0004	−0.0029	−0.0049
H(14B)	0.0310	0.0239	0.0173	−0.0072	−0.0010	−0.0064
H(14C)	0.0219	0.0265	0.0160	0.0016	−0.0029	−0.0049
H(15A)	0.0257	0.0393	0.0132	0.0025	0.0058	−0.0018
H(15B)	0.0321	0.0271	0.0130	−0.0038	0.0032	−0.0008
H(15C)	0.0292	0.0263	0.0128	0.0034	0.0028	−0.0027

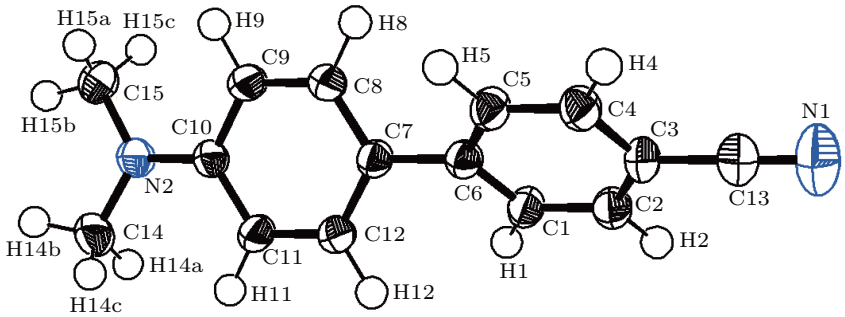

Fig. 3. (color online) ORTEPIII diagram of the DMACB molecule with atomic labeling scheme.

6. Electron-density maps

The aspherical atom model used in multipolar refinement gives structure factor phases closer to the true phases than the spherical or independent atom model does.[30,31] This enables the mapping of the electron density by Fourier synthesis in various ways using the program XDGRAPH implemented in the XD program package.[15]

The experimental density deformation map is shown in Fig. 4, from which we can notice the absence of the density on the atomic sites and the appearance of all the bond density peaks. This map confirms the high quality of the data sets and the efficiency of the formalism used for the data processing as proposed by Blessing.[18] This visualization is obtained using the calculated multipole phases with the observed structure factors $F_{\rm obs}(h)$

$$\delta\rho^{\rm exp}(r) = \frac{1}{V}\sum_h [|F_{\rm obs}(h)|\,{\rm e}^{{\rm i}\phi_{\rm mul}} - |F_{\rm sph}(h)|\,{\rm e}^{{\rm i}\phi_{\rm sph}}]\,{\rm e}^{-2\pi {\rm i} hr}, \quad (3)$$

where $F_{\rm sph}(h)$ is computed with atomic positions and thermal parameters. The experimental density map from high-order refinement is $\rho_{\rm exp} = \rho_{\rm o} - \rho_{\rm sph}$, where $\rho_{\rm o}$ is the observed electron density and $\rho_{\rm sph}$ is the calculated electron density using the atomic parameters obtained from the high-order refinement.

We have explored four planes to visualize the electron density distribution: the plane of the aromatic cycle containing the C(1), C(2), C(3), C(4), C(5) and C(6) atoms; the plane of the second aromatic cycle containing the C(7), C(8), C(9), C(10), C(11) and C(12) atoms; the third plane formed by the elctro-donor group (amino dimethyl); and the last plane containing the elctro-acceptor goup (cyano). Figure 4 gives the different maps cited above, all contour intervals are 0.05 e·Å^{-3}.

We observe that the electron density distribution is almost centered in the middle of the chemical bonds. We also notice that the peaks (Fig. 4(d)) of the electron density in the connection N(2)–C(14) and N(2)–C(15) are centered towards the nitrogen N(2) backing the electro donor character of the methyl

group. The symmetrical electron distribution along both sides of the C(13)–N(1) axis shows clearly the multi bonding aspect of the C(13)–N(1) chemical bond.

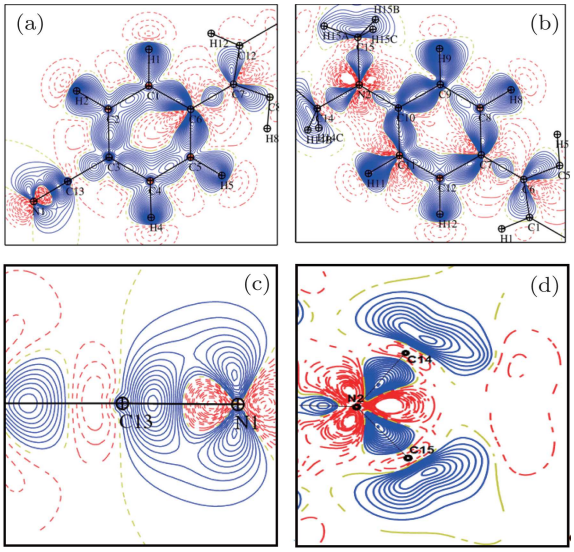

Fig. 4. (color online) Deformation density map with a contour interval of 0.05 e·Å^{-3}, positive density in red and negative density in blue: (a) the plane of the first aromatic cycle; (b) the plane of the second aromatic cycle; (c) the plane of the cyano group; (d) the plane of dimethyl amino group.

7. Conclusion

The *ab initio* theoretical structure investigation leads to an optimized molecule with bond lengths and bond angles closer to the X-ray experiment results. No significant structural changes are observed compared to the previous results obtained at room temperature. However, the thermal motion analysis using the Hirshfeld rigid-bond test shows the advantages of the very low temperature data collection. The atomic motions have been significantly reduced. The maximum discrepancy is only 0.0005 Å^2 after the multipolar refinement.

The multipolar model of Hansen and Coppens allows us to obtain the electron charge density function. In order to check the quality of our analysis, we have used the obtained density function to visualize the electron charge density distribution around the different atoms.

We have explored systematically the main molecule planes. The different sections show clearly the accumulation of the electron charge density along the chemical bonding. The oxygen lone pairs have been perfectly localized. The good quality of the obtained results can only confirm the accuracy of the obtained charge density function, which will lead us in our next step in a forthcoming paper to the calculation of the molecular dipole moment and the electrostatic potential around the molecule in order to confirm the nature of electron charge transfer of the DMACB compound.

References

[1] Bredas J L, Adant C, Tackx P, Persoons A and Pierce B M 1994 *Chem. Rev.* **94** 243

[2] He M, Leslie T M, Sinicropi J A, Garner S M and Reed L D 2002 *Chem. Mater.* **14** 4669

[3] Locatelli D, Quici S, Roberto D and De Angelis F 2005 *Chem. Commun.* **43** 5405

[4] Kang H, Facchetti A, Jiang H, Cariati E, Righetto S, Ugo R, Zuccaccia C, Macchioni A, Stern C L, Liu Z, Ho S T, Brown E C, Ratner M A and Marks T J 2007 *J. Am. Chem. Soc.* **129** 3267

[5] Hu Y Y, Sun S L, Zhong R L, Xu H L and Su Z M 2011 *J. Phys. Chem. C* **115** 18545

[6] Zyss J 1994 *Molecular Nonlinear Optics: Materials, Physics and Devices* (New York: Academic Press)

[7] Nalwa H and Miyata S 1996 *Nonlinear Optics of Organic Molecules and Polymers* (New York: CRC Press)

[8] Ledoux I and Zyss J 1997 *Molecular Nonlinear Optics: Fundamentals and Applications* (Khoo I C, Simoni F, Umeton C, Ed.) pp. 1–48

[9] Andraud C, Zabulon T, Collet A and Zyss J 1999 *Chemical Physics* **245** 243

[10] Zhou Z J, Li X P, Ma F, Liu Z B, Li Z R, Huang X R and Sun C C 2011 *Chem. Eur. J.* **17** 2414

[11] Bureš F, Schweizer W B, May J C, Boudon C, Gisselbrecht J P, Gross M, Biaggio I and Diederich F 2007 *Chem. Eur. J.* **13** 5378

[12] Bureš F, Schweizer W B, Boudon C, Gisselbrecht J P, Gross M and Diederich F 2008 *Eur. J. Org. Chem.* **6** 994

[13] May J C, Biaggio I, Bureš F and Diederich F 2007 *Appl. Phys. Lett.* **90** 251106

[14] Bureš F, Pytela O and Diederich F 2009 *J. Phys. Org. Chem.* **22** 155

[15] Zyss J, Ledoux I, Bertault M and Toupet E 1991 *Chemical Physics* **150** 125

[16] Hansen N K and Coppens P 1978 *Acta Cryst. A* **34** 909

[17] Koritsanszky T, Howard S, Richter T, Su Z, Mallinson P R and Hansen N K 2003 *XD a Computer Program Package for Multipole Refinement and Analysis of Electron Densities from Diffraction Data* (Berlin: Free University of Berlin)

[18] Blessing R H 1989 *J. Appl. Cryst.* **22** 396

[19] *International Tables for X-ray Crystallography* Vol. C 1999 (New York: Kluwer Academic Publishers)

[20] Stewart R F, Davidson E R and Simpson W T 1965 *J. Chem. Phys.* **42** 3175

[21] Becker P J and Coppens P 1974 *Acta Cryst. A* **30** 129

[22] Frisch M J, Trucks G W, Schlegel H B *et al.* 2003 *Gaussian 03* (Pittsburgh, Gaussian 03 Revision A.1)

[23] Trueblood K N 1990 *Program THMA11* (Los Angeles: Department of Chemistry and Biochemistry, University of California)

[24] Hirshfeld F L 1976 *Acta Cryst. A* **32** 239

[25] Hirshfeld F L 1971 *Acta Cryst. B* **27** 769

[26] Hirshfeld F L 1977 *Theor. Chim Acta* **44** 129

[27] Hirshfeld F L and Hope H 1980 *Acta Cryst. B* **36** 406

[28] Baert F, Schweiss P, Heger G and More M 1988 *J. Mol. Struct.* **178** 29

[29] Johnoson C K 1965 *ORTEP Program Report ORNL-3794* (Tennessee: Oak Ridge National Laboratory)

[30] Coppens P 1997 *X-ray Charge Densities and Chemical Bonding* (New York: Oxford)

[31] Souhassou M and Blessing R H 1999 *J. Appl. Cryst.* **32** 210